

The effect of using ramps with trench cylindrical holes on film cooling effectiveness

Dr. Ahmed A. Imram
Lecturer
Mechanical Eng. Dept.
University of Technology

Humam K. Jalghef
Asst. Lecturer
Mechanical Eng. Dept.
University of Technology

Dr. Falah F. Hatem
Lecturer
Mechanical Eng. Dept.
University of Technology

Abstract:

The effect of introducing ramp with a cylindrical slot hole on the film cooling effectiveness has been investigated experimentally and numerically. The film cooling effectiveness measurements are obtained experimentally. A test study was performed at a single mainstream with Reynolds number 76600 at three different coolant to mainstream blowing ratios 1.5, 2, and 3. Numerical simulation is introduced to primarily estimate the best ramp configurations and to predict the behavior of the transport phenomena in the region linked closely to the interaction between the coolant air injection and the hot air mainstream flow. The results showed that using ramps with trench cylindrical holes would enhanced the overall film cooling effectiveness by 83.33% compared with baseline model at blowing ratio of 1.5, also the best overall film cooling effectiveness was obtained at blowing ratio of 2 while it is reduced at blowing ratio of 3.

Keywords: Film Cooling, Effectiveness, Trench, Ramp.

تأثير استخدام المنحدرات مع الشق القوسي المثقب على فعالية التبريد الغشائي

الخلاصة:

تم دراسة تأثير إدخال المنحدرات مع وجود شق أسطواني يحتوي على ثقوب على فعالية التبريد الغشائي عمليا ونظريا. يتم الحصول على قياسات فعالية التبريد الغشائي تجريبيا. وأجريت دراسة اختبار في التيار واحد من رقم رينولدز 76600 مع ثلاث سرع مختلفة للهواء البارد لتحقيق نسبة نفث (1.5 و 2 و 3) تقدم المحاكاة العددية مبدئيا لتخمين أفضل التشكيلات للمنحدرات والتنبؤ بسلوك ظاهرة الانتقال في المنطقة القريبة جدا "من تداخل الهواء البارد المحقون مع المجرى الرئيسي للهواء الحار . أظهرت النتائج أن استخدام المنحدرات مع الشق القوسي لثقوب الأسطواني من شأنه تعزيز فعالية التبريد الغشائي بنسبة 83.33% مقارنة مع النموذج الأساسي لنسبة نفث 1.5, كذلك أفضل فعالية للتبريد الغشائي تم الحصول عليها عند نسبة نفث 2 في حين قلت فعالية التبريد عند نسبة نفث 3.



Nomenclature

D	hole diameter (mm)
K	turbulent kinetic energy (m^2/s^2)
k	thermal conductivity of test surface material ($\text{W}/(\text{mK})$)
Re	mainstream Reynolds' number based on hole diameter
T	temperature (K)
U	velocity (m/s)
x, y and z	Cartesian coordinate axes
X	streamwise distance along the test plate (mm)
Y	distance normal to the test plate surface (mm)
Z	pitch wise distance (mm)

Greek Symbols

α	thermal diffusivity of the test surface material (m^2/s)
η_{sa}	spanwise averaged film cooling effectiveness
η_o	overall area- averaged film cooling effectiveness
μ	Viscosity of air ($\text{kg}/\text{m.s}$)
ε	dissipation rate of turbulent kinetic energy (m^2/s^3)
ρ	density (kg/m^3)

Subscripts

<i>c</i>	coolant
<i>I</i>	initial
<i>f</i>	Film
<i>m</i>	mainstream

Abbreviations

BR	blowing ration $\left(\frac{\rho_c U_c}{\rho_m U_m}\right)$
CFD	computational fluid dynamics
CRVP	counter-rotating vortex pairs

1. Introduction

Film cooling is used to protect surfaces faced high temperature such as that exist in the combustor, gas turbine blades and many other parts, by injection of coolant fluid at a lower temperature than that of the main flow to flood the surfaces to be protected. Cohen [1] stated that the advanced gas-turbine stages are designed to operate at increasingly higher inlet temperatures to increase thermal efficiency and specific power output. This increase is made possible by advances in materials such as super alloys and thermal-barrier coatings and by cooling technology such as internal impingement cooling. The inlet temperatures can far exceed allowable material temperatures by using cooling. The principle of film cooling involves injection of coolant mainly compressed air from the compressor through the film holes to form a thin thermal barrier layer to protect the blade surface of the hot gases mainstream flow. The objective of film cooling is to achieve a low heat transfer from the surrounding hot mainstream to the surface to be protected. In the recent years, several studies have been focused on



developing the hole shape and its configurations to enhance film cooling effectiveness. Film cooling research on a flat surface is common, flat surface models can be used to study the effects of individual parameters with relative ease and are less expensive. Studies have proved that the results obtained on simple flat surface models can be applied to real engine designs with slight corrections.

Many researchers studied the effects of design and operating parameters on film cooling at which the coolants injected from one or many rows of inclined holes. The studied parameters include the hole shapes, film-cooling hole inclination, length-to-diameter ratio, spacing between holes, turbulence and embedded vortices in the mainstream flow. Hyams et al. [2] and Bunker [3] provided a comprehensive review of the research on hole shape they conclude that fan-shape hole is more efficient than cylindrical shape. Zaman and Foss [4] and Zaman. Ekkad et al. [5] showed that placing tabs on the upstream side of the film-cooling hole exit can improve film-cooling effectiveness. Bunker [6] proposed creating a trench about a row of film cooling holes to modify the coolant-mainstream interactions. Altorairi [7] shows that the holes embedded in trench give quite useful improving of film-cooling effectiveness. Sangkwon and Shih [8] presented, by using commercial CFD software FLUENT, they proposed a geometry modification upstream of the cylindrical holes by using upstream ramps to modify the approaching boundary layer flow and its interaction with the film cooling jets. The results obtained showed that there are increasing about two or more times higher than that without the ramp in the film cooling effectiveness. Assim et al. [9] investigated experimentally the effect of introducing ramps with conical holes on film cooling performance. The results show that film's effectiveness is greatly enhanced when using ramps, they also show that the double ramped-hole model provides promising film cooling performance particularly at moderate and high blowing ratios. Humam [10] study the effect of embedded hole in arc trench, the results show that this geometry arrangement will improve the performance of film cooling especially at low blowing ratios. The present work investigation of use the ramp with cylindrical slot to improving the film cooling effectiveness.

2. Experimental setup and procedure

The experimental apparatus was consisted of two open loops, mainstream and coolant air flow loops as shown in Fig. (1). The settling chamber of the test rig contains series rows of electrical heaters, row of honeycomb, and screens to ensure an adequate hot air of uniform velocity and temperature throughout the test rig. The mainstream routed through a convergent- divergent contraction having a rectangular cross-section before flowing through the test section. The bottom wall of the test section considered as a testing plat model, the model made by (234mmx123mm) Plexiglass plate of 1cm thickness Fig. (2) shows the testing plate with ramp-trench hole arrangement. In order to allow the air to reach the desired temperature, the air is initially routed out away from the test section by using a by-pass gate passage. The temperature of the mainstream is continuously monitored at the exit of the gate and when the desired temperature is reached, the gate is gradually fully opened. Centrifugal air blower was used to supply the cooled air to the plenum. The plenum is located below the test model as shown in Fig.1. The coolant air enters a plenum then ejected through holes in the test section. The coolant air pressure was measured at the inlet of the test section.



Digital thermometers are used to measure the mainstream and coolant air temperature. Pre-testing shows that all holes ejected constant desired flow rate and temperature. The mainstream temperature adjusted with a laboratory temperature (ambient air drawn by a blower) to give highest limit of $(T_c/T_h=0.4)$. The infrared thermography system (Fluke Ti32) is used to measure surface temperatures. The thermal image can be displayed using standard color palettes or Ultra Contrast TM color palettes. The IR system is greatly affected by both background temperature and local emissivity. The test surface was sprayed with mat black color to increase the emissivity as a perfect black body. The temperature measurement taken is not accurately recorded unless the IR system is calibrated. The system is calibrated by measuring the temperature of the test surface using thermocouple type K and the reading of the IR camera. The test surface is heated by mainstream hot air. The measured of temperatures obtained by both ways and they are recorded and stored during the heating process until achieving a steady state condition. Due to the emissivity of the test surface temperature is obtained by IR camera is different from the temperature obtained by the thermocouple; therefore IR camera reading is adjusted until both temperature readings are matched. The system, calibration of the temperature range in the present work is taken between -10°C and $+80^{\circ}\text{C}$, this calibration was automatically in the IR camera.

2. Numerical simulation

Computational fluid dynamics (CFD) by using ANSYS Fluent Package is presented as a technical help to visualization the experimental tests. Also to predict the behavior of the transport phenomena in the region link closely to the interaction between the coolant injection and the mainstream flow.

In the present study, air is taken as the working fluid and the flow characteristics are assumed to be as follows,

- Steady flow, Three dimensional
- Newtonian fluid
- Incompressible fluid
- Turbulent flow

The solid model of the hole assembly is shown in Fig. (3). The blowing ratio (BR) was based on measured total coolant mass flux and hot mainstream air as:

$$BR = \left(\frac{\rho_c U_c}{\rho_m U_m} \right) \quad (1)$$



The time-averaged, steady state Navier-Stokes equations as well as equations for mass and energy are solved. The governing equations for conservation of mass, momentum, and energy are given as:

$$\frac{\partial}{\partial x}(\rho u_i) = S_m \quad (2)$$

$$\frac{\partial}{\partial x}(\rho u_i u_j) = \rho \bar{g}_j - \frac{\partial p}{\partial x_i} + \frac{\partial}{\partial x_i}(\tau_{ij} - \rho \overline{u_i u_j}) + F_j \quad (3)$$

$$\frac{\partial}{\partial x}(\rho u c_p u_i T) = \frac{\partial}{\partial x_i} \left(\lambda \frac{\partial T}{\partial x_i} - \rho c_p \overline{u_i T} \right) + \mu \phi + S_h \quad (4)$$

Where τ_{ij} is the symmetric stress tensor defined as:

$$\tau_{ij} = \mu \left(\frac{\partial u_j}{\partial x_i} + \frac{\partial u_i}{\partial x_j} - \frac{2}{3} \delta_{ij} \frac{\partial u_k}{\partial x_k} \right) \quad (5)$$

$(\mu \phi)$ Is the viscous dissipation, and λ is the thermal conductivity. The terms of $\rho \overline{u_i u_j}$ and $\rho c_p \overline{u_i T}$ represent the Reynolds stresses and turbulent heat fluxes, respectively, which should be modeled properly for a turbulent flow. Two additional transport equations for the turbulence kinetic energy (k) and the turbulence dissipation rate (ϵ) are solved. The standard ($k - \epsilon$) model is economical with reasonable accuracy for a wide range of turbulent flows and it is widely used in heat transfer simulation.

The Boussinesq hypothesis is used in the ($k - \epsilon$) model and the advantage of this approach is the relative low computational cost. In the ($k - \epsilon$) model, two additional transport equations for the turbulent kinetic energy (k) and turbulent dissipation rate (ϵ) are solved and the eddy viscosity (μ_t) is computed as a function of k and ϵ . The standard ($k - \epsilon$) model [11], is a semi-empirical model based on model transport equations for the turbulent kinetic energy (k) and its dissipation rate (ϵ). Assumed that the flow is fully turbulent, and the effects of molecular viscosity are negligible, the turbulence kinetic energy (k) and its dissipation rate (ϵ) are obtained from the following equations [12]:

$$\frac{\partial}{\partial x_i} \rho k u_i = \frac{\partial}{\partial x_j} \left[\left(\mu + \frac{\mu_t}{\sigma_k} \right) \frac{\partial k}{\partial x_j} \right] + G_k + G_b - \rho \epsilon + Y_M + S_k \quad (6)$$

$$\frac{\partial}{\partial x_i} \rho \epsilon u_i = \frac{\partial}{\partial x_j} \left[\left(\mu + \frac{\mu_t}{\sigma_\epsilon} \right) \frac{\partial \epsilon}{\partial x_j} \right] + C_{1\epsilon} \frac{\epsilon}{k} (G_k + C_{3\epsilon} G_b) - C_{2\epsilon} \rho \frac{\epsilon^2}{k} + S_\epsilon \quad (7)$$

Turbulent viscosity (μ_t) is computed as a function of (k) and (ϵ).

$$\mu_t = \rho C_\mu \frac{k^2}{\epsilon} \quad (8)$$



The generation of turbulence kinetic energy due to the mean velocity gradients (G_k) is computed by:

$$G_k = -\rho \bar{u}_i \bar{u}_j \frac{\partial u_i}{\partial x_j} \quad (9)$$

The generation of turbulence kinetic energy due to the buoyancy (G_b) can be neglected. Y_M represents the contribution of the fluctuating dilatation in compressible turbulence to the overall dissipation rate, ($C_{1\varepsilon}$), ($C_{2\varepsilon}$), and (C_μ) are taken as the default values ($C_{1\varepsilon}=1.44$, $C_{2\varepsilon}=1.92$, and $C_\mu=0.09$) in FLUENT [14]. (σ_k) and (σ_ε) are the turbulent Prandtl numbers for (k) and (ε) taken as 1 & 1.3, respectively. (S_k) and (S_ε) are user-defined source terms [13]. The term (λ) in the energy equation (3) is the effective thermal conductivity which is given by:

$$\lambda = k + \frac{c_p \mu_t}{Pr_t} \quad (10)$$

The film cooling effectiveness is essentially a non-dimensional temperature given as:

$$\eta = \frac{T_m - T_w}{T_m - T_c}$$

3.1 Mesh Generation

There are mainly two types of approaches in volume meshing, structured and unstructured meshing. FLUENT can use grids comprising of tetrahedron or hexahedron cells in three dimensions. The type of mesh selection depends on the application. Unstructured grids are in general successful for complex geometries, so for this reason the unstructured tetrahedron grids was used in the current study.

Although many mesh generation codes, FLUENT and ANSYS, support mesh generation of solid geometry and three-dimensional models from a single phase with minimum input from the user, but it is more durable to divide this process into subsequent steps including two major issues for further controlling of the mesh. These have included the followings [14]:

I) Surface mesh generation

Surface mesh is created for cylinder (tube), hot bottom surface of hot box and upper surface of the coolant box, and other boundaries as in the following:

- Edges are meshed by assigning an interval size for each boundary comprising a closed loop of area.
- Meshed edges are controlled by specifying a grading scheme for each individual edge.
- Once all edges are meshed, a triangular element is used to generate a three - dimensional pave unstructured surface mesh.



II) Volume mesh generation

As far as all the surfaces have been meshed for each individual area, now volume mesh can be created for each zone comprising a closed loop of area using T-Grid. Building the mesh requires fine cells in area near the bottom surface of hot box and cylinder tube. Therefore, the mesh should be manipulated and controlled manually to keep smooth mesh transition and maintain accurate mesh for a three-dimensional model with a minimum computational expense. This is achieved by applying the size function. Size functions are used to control the size of mesh intervals for edges and mesh elements for faces or volumes and thus to keep smooth transition of mesh from fine mesh near bottom surface of hot box and cylinder and upper surface to coarse mesh far away at the undisturbed boundaries as shown in Figure (4).

3.2 Boundary Conditions

At all boundaries except those denoted as "main inlet", "coolant inlet", "exit", and symmetry boundary conditions shown in Fig.3, an adiabatic wall boundary condition is used. At the "main inlet," a velocity-inlet boundary condition is specified by x-velocity equal to 20 m/s, and all other components equal to zero. The temperature is given as 323K at the main inlet. The turbulence intensity and hydraulic diameter (which is used to determine the turbulence length scales) are specified as 2% and 24 mm, respectively. The plenum inlet mass flow rate was adjusted to produce the blowing ratio desired and the inlet temperature of the coolant is 298K to match the coolant to freestream density ratio (DR) of 1.09 with experiments. The turbulence intensity and hydraulic diameter are specified as 3% and 23mm, respectively. At the "exit", a pressure-outlet boundary condition is specified with a gage pressure equal to zero (giving an absolute pressure of 101.325 Pa).

3- Results and Discussions

The experimental results of the present model are compared with a baseline model (ordinary cylindrical hole) which has been tested by Lu et al. [15] at blowing ratio of 1.5 is given by Fig.5 which compares the distribution of spanwise averaged film cooling effectiveness (η_{sa}) along the normalized streamwise distance (X/D). It seems that the spanwise averaged film cooling effectiveness along the (X/D) of the present model is better than that of the baseline model, this can be explained by the numerical results as shown in Fig. (6), the presence of the ramp in front the hole is damped the interaction between the mainstream and the coolant stream, so there is an delays of the entrainment of hot gases by the counter-rotating vortex pairs (CRVP) in the film-cooling jets and reduces the effect of CRVP. At blowing ratio of 1.5, the overall film cooling effectiveness is enhanced by 92 % as compared with baseline model. Figure (6) shows the experimental results of span wise averaged film cooling effectiveness along the normalized stream wise distance (X/D) for different blowing ratios (1.5, 2, and 3), the model provides the best span wise averaged film cooling effectiveness at blowing ratio of 2. These remarkable results are verified by the results presented in Fig. (8).

Effect of blowing ratios in the overall area-averaged film cooling effectiveness is presented in this figure in the present model. We can note that the overall film cooling effectiveness reduce notably at $BR=3$, the reason return to increase the vortices due to the high momentum of injection coolant air and interaction with mainstream. The enhancement in the film cooling effectiveness between the present model and baseline model return to used the new two type of configuration which is ramp and cylindrical slot which is give the chance to coolant air in go away in forward direction without create the vorticity which is allowed to the hot air to reach into the surface that we wanted to protect.

5. Conclusion

- 1- The overall film cooling effectiveness enhanced by 83.33% compared with a baseline model at a blowing ratio of 1.5.
- 2- The best overall film cooling effectiveness has been feted at a blowing ratio of 2.
- 3- The present model did not give a good performance of the effectiveness at blowing ratio of 3.
- 4- use the present configuration of ramp in the upstream injection holes give the advance in avoiding the impact interaction between the mainstream and injection air.
- 5- used the present design of ramp with cylindrical slot give the time to the coolant injection air in bath arrangement.

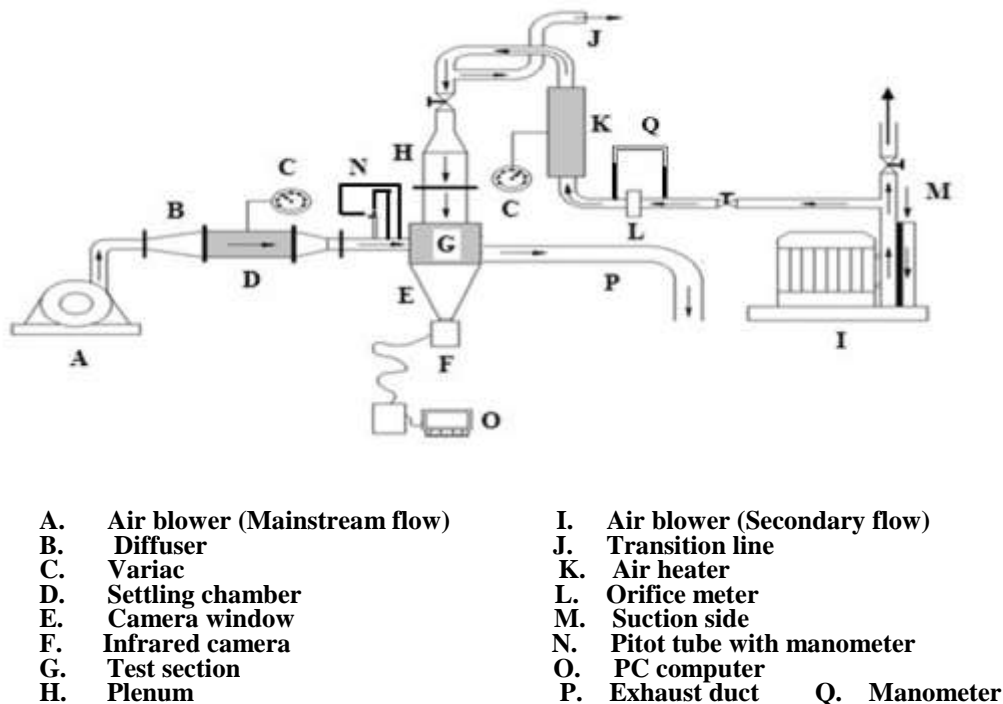


Fig. (1) Experimental test rig detail

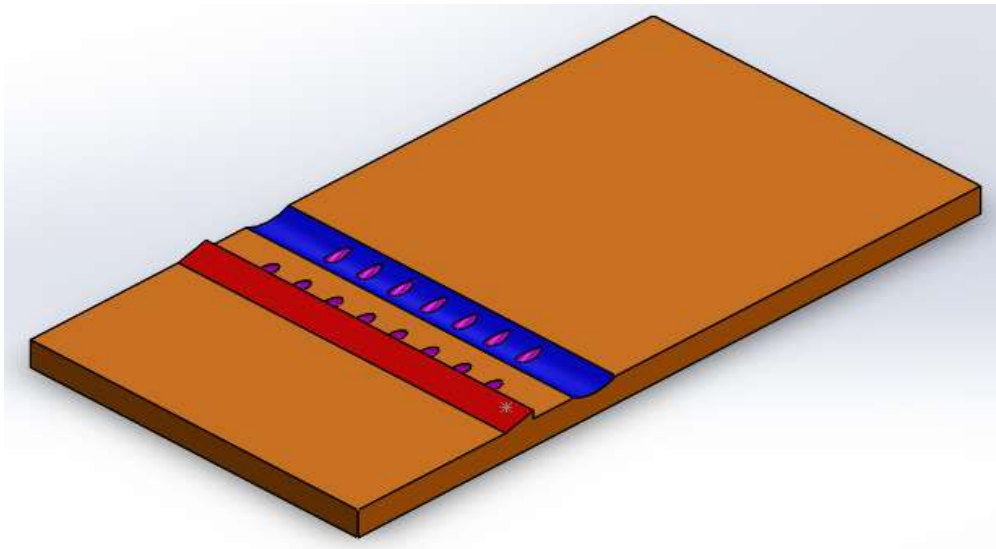


Fig. (2) Testing plate shape

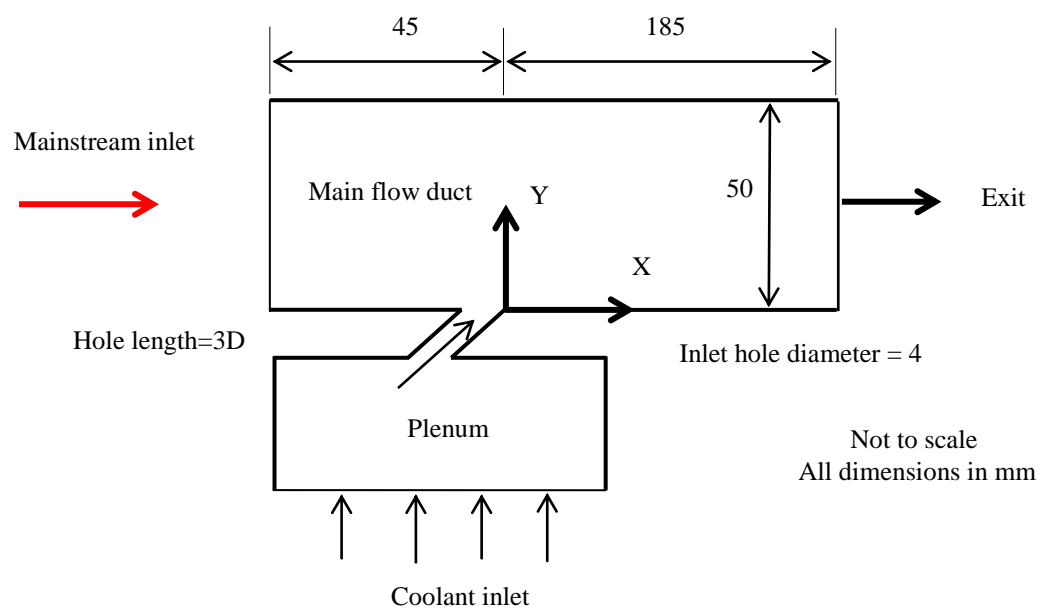


Fig. (3) Boundary conditions

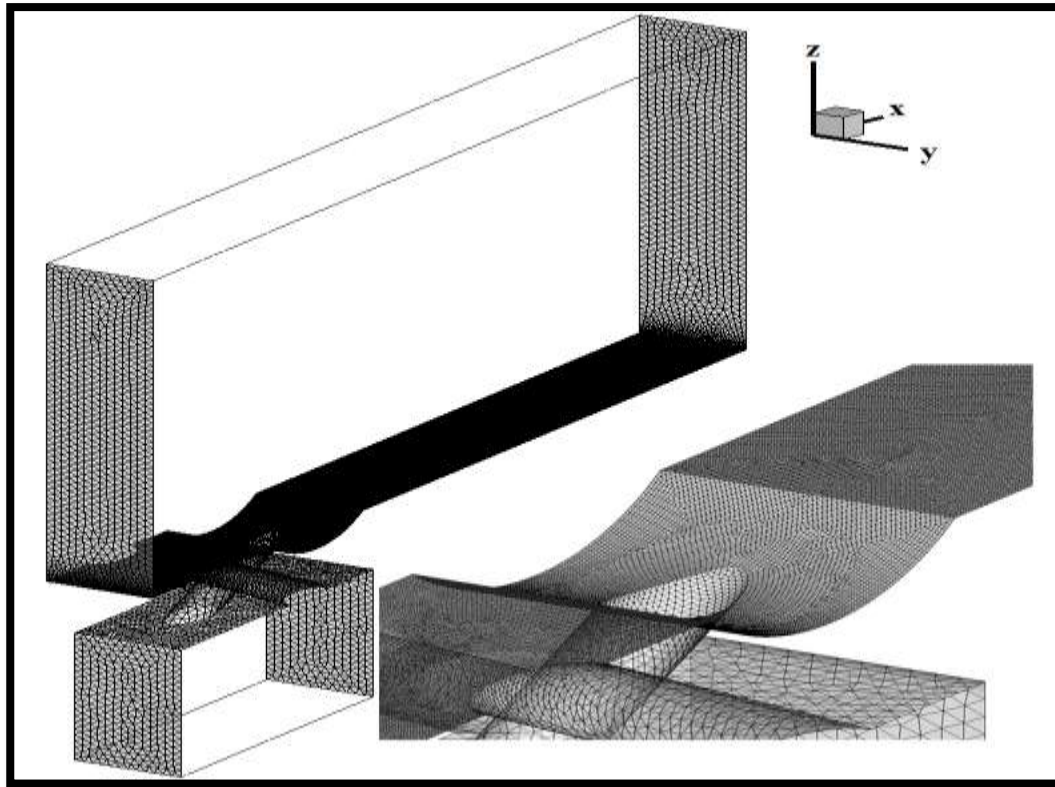


Fig. (4) Tetrahedral mesh distribution for film cooling system

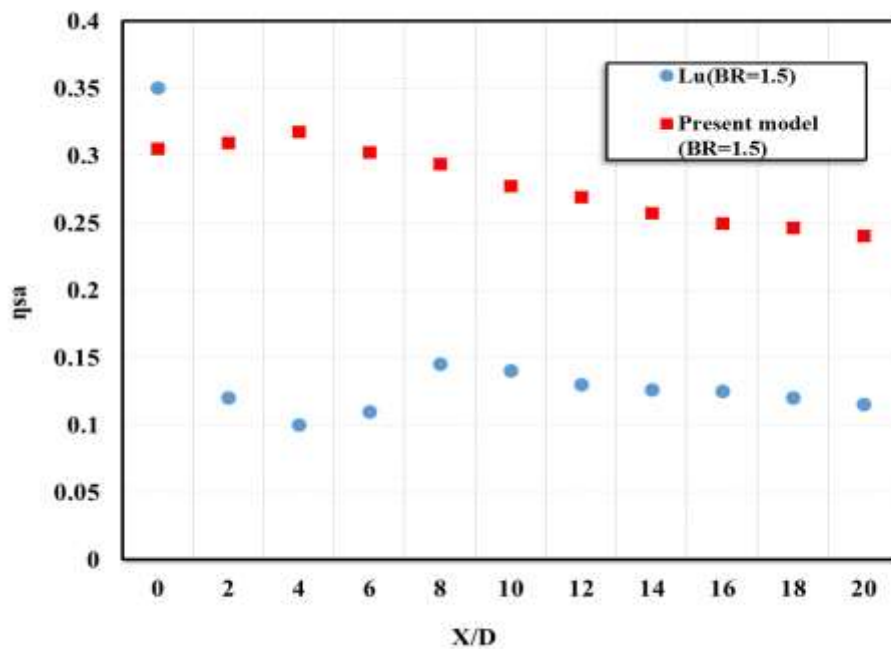


Fig. (5) Variation of spanwise averaged film cooling effectiveness (η_{sa}) with (X/D) for baseline model and present model at BR=1.5

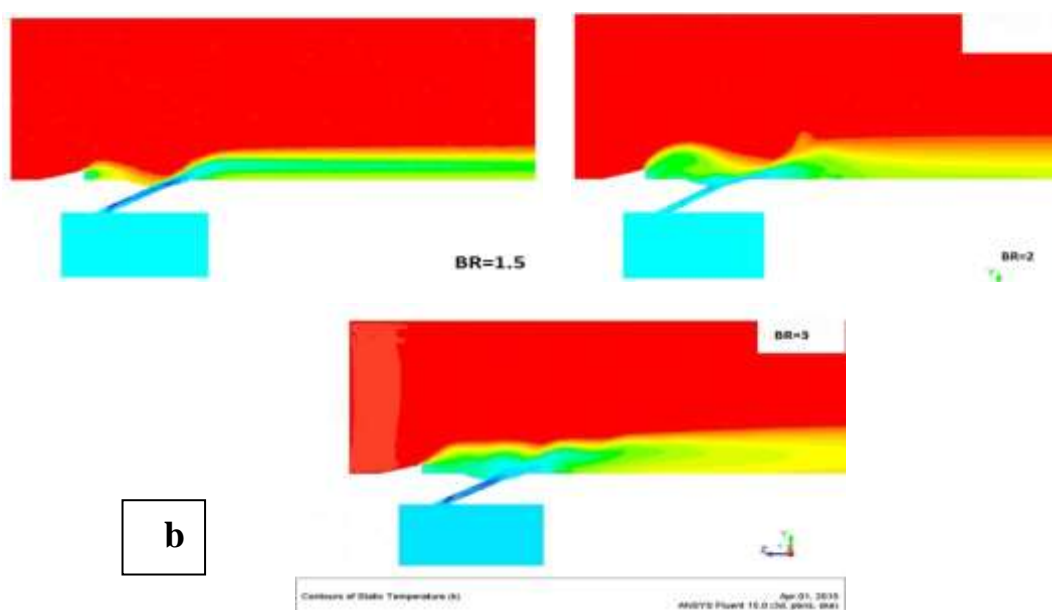
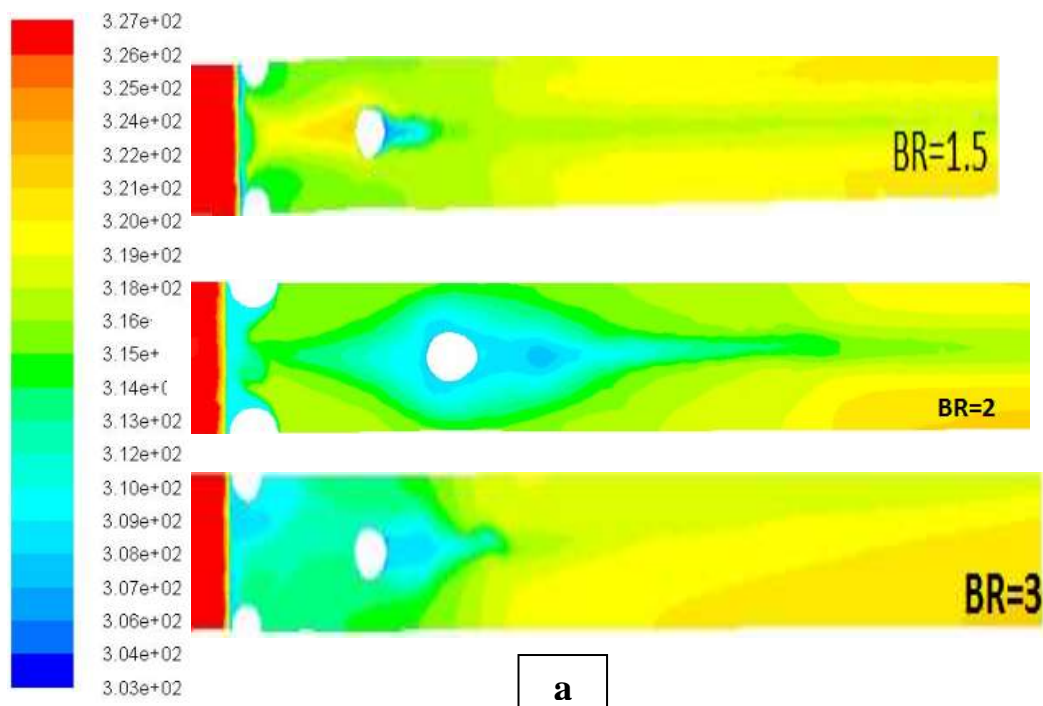


Fig. (6) Numerical results of the present model
 (a) temperature contours of bottom surface.
 (b) temperature contours of the all test suction.

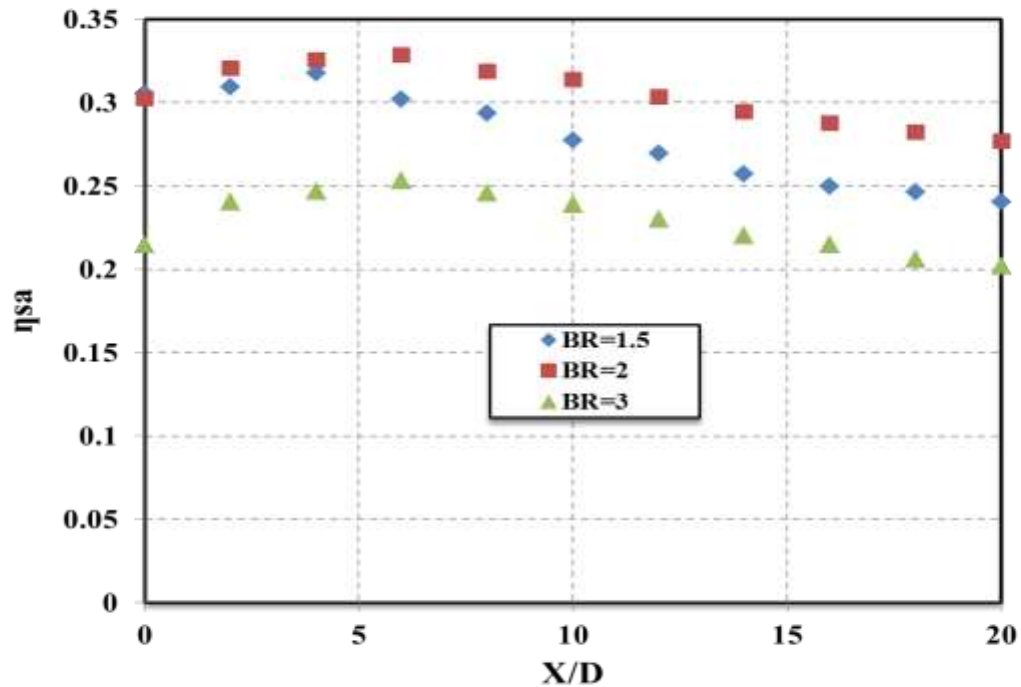


Fig.(7): Variation of spanwise averaged film cooling effectiveness (η_{sa}) with (X/D) at different blowing ratio. (Experimental)

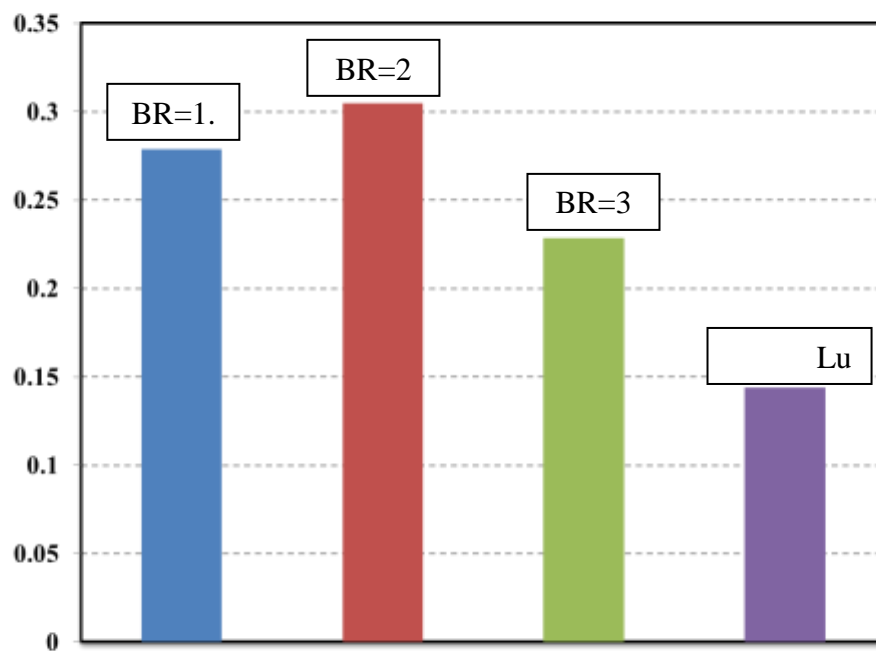


Fig.(8): Effect of blowing ratio on the overall film cooling effectiveness (η_o). (Experimental)



6. References

- [1] Cohen H., Rogers G.F.C., Saravanamuttoo H.I.H., 1996, "Gas Turbine Theory", 4th edition, Longman House, Burnt Mill, England .
- [2] D. G. Hyams, K. T. McGovern, J. H. Leylek, "Effects of geometry on slot-jet film cooling performance", ASME Paper No. 96-GT-187 (1997).
- [3] R. S. Bunker, "A review of shaped hole turbine cooling technology", ASME J. Heat Transfer, 127 (2005) 441–453.
- [4] K. B. M. Q. Zaman, J. K. Foss, "The effects of vortex generators on a jet in a cross-flow", Phys. Fluids, 9(1), (1997) 106–114.
- [5] S. V. Ekkad, H. Nasir, S Acharya, "Flat surface film cooling from cylindrical holes with discrete tabs", J. Thermophys. Heat Transfer 17(3) (2003) 304–312.
- [6] R. S. Bunker, "Film cooling effectiveness due to discrete holes within transverse surface slots", Proceedings IGTI Turbo Expo, Amsterdam, the Netherlands, ASME Paper No. GT-2002–30178 (2002).
- [7] M. S. Altorairi, "Film cooling from cylindrical holes in transverse slots", MSc. thesis, Louisiana State University (2003), Baton Rouge, LA, USA.
- [8] Sangkwon, Na. and Shih, T. I-P. , "Increasing Adiabatic Film-Cooling Effectiveness by Using an Upstream Ramp", Journal of Heat Transfer, Vol.129, pp. 464-470, 2007.
- [9] Assim. H. Yousif, . Kutaeba J. AL-Khishali, and Falah F. Hatem, "Film cooling experimental investigation for ramped-conical holes geometry", International Journal of Scientific & Engineering Research, Volume 4, Issue 11, November 2013.
- [10] Humam K. Jalghaf, " Study the Effect of Holed Arc Trench of Compound Orientation Angle on Surrounding Flow Field and Film Cooling Performance", M.Sc. thesis, University of Technology-Baghdad, 2013.
- [11] Launder B.E., and Spalding D.B., "The Numerical Computation of Turbulent Flows", Computer Methods in Applied Mechanics and Engineering, Vol. 3, pp. 269-289, 1974.
- [12] Launder, B. E., and Spalding, D. B., "Lectures in Mathematical Models of Turbulence", Academic Press, London, England, 1972.
- [13] Fluent 12 User's Guide, programing and Tutorial Guide, Version 12, Ansys Inc, 2009.
- [14] Fluent 12 User's Guide, programing and Tutorial Guide" Fluent, Version12, AnsysInc, 2009.[15] Lu, Y., Allison, D., and Ekkad, S.V., 2007, "Turbine blade showerhead film cooling: Influence of hole angle and shaping", International Journal of Heat and Fluid Flow, USA, Vol. 28.